Cocrystallization Phenomenon between the H and D Species of *Isotactic* Polypropylene Blends As Revealed by Thermal and Infrared Spectroscopic Analyses for a Series of D/H Blend Samples

Kummetha Raghunatha Reddy,[†] Kohji Tashiro,*[,†] Takashi Sakurai,[‡] and Noboru Yamaguchi[‡]

Department of Future Industry-oriented Basic Science and Materials, Toyota Technological Institute, Tempaku, Nagoya 468-8511, Japan, Petrochemicals Research Laboratory, Sumitomo Chemical Co. Ltd. Kitasode, Sodegaura, Chiba 299-0295, Japan

Received August 9, 2008; Revised Manuscript Received October 13, 2008

ABSTRACT: Cocrystallization phenomenon between the hydrogenous (H) and deuterated (D) species of a series of isotactic polypropylene blends with various D/H contents has been established for the first time on the basis of the detailed analysis of thermal and infrared spectral data for both α1 and α2 crystalline forms, where the α1 form is the crystal form of disordered chain packing mode but the α2 form has the ordered chain packing structure. The melting point has been found to shift continuously towards higher temperature side with an increase in the H component. This continuous change in the melting and crystallization point was reasonably interpreted by assuming the coexistence of D and H chain stems in the crystal lattice. The so-called correlation splitting was detected as doublets of the infrared bands for the pure D species sample at around 1066 cm^{-1}. This correlation band splitting width changed systematically depending on the D/H ratio and became a singlet for the sample with only 5 mol % D component. This systematic change in the splitting width of the infrared bands can be interpreted also reasonably based on the concept of the random existence of D and H chain stems in the crystal lattice. Although the details of the thermal behavior and the infrared band splitting are different between the α1 and α2 forms, the observed phenomena are essentially the same each other. Both of thermal and infrared data indicate reasonably the cocrystallization phenomenon of the D and H chain stems in the crystal lattice of the α1 and α2 forms when cooled from the melt, suggesting a possibility of the random chain folding mode in the crystalline lamellae.

Introduction

Semicrystalline polymers show complex microstructure or higher order structure consisting mainly of crystalline lamellae and amorphous region. To improve the physical properties of the semicrystalline polymers, it is essential to control the higher order structure in a systematic way. For this purpose, we need to reveal the aggregation state of molecular chains as well as the formation of such structure in molecular level. In particular, to understand the structural evolution process from the melt or the crystallization process it is important to clarify the behavior of individual chains during the formation of lamellae and to find out the trace of these chains passing through the crystalline and amorphous regions.[1,2]

To trace the single chain behavior in the crystallization phenomenon, the so-called labeling method is employed as one of the most useful methods where a small amount of chains are labeled by isotope (deuterium) and mixed together in the unlabeled polymer matrix. This labeling method is based on such an idea that the vibrational frequency and neutron scattering length of the deuterated (D) species are different from those of hydrogenated (H) species.[3−14] In the actual experiments we assume that the D and H chains behave in almost the same manner in the crystallization process. But this assumption is not always reasonable depending on the polymer sample under the study. For example, in the case of polyethylene, many experiments have been reported about the blends between H and D species to reveal the trace of D (or H) chains in the H (or D) matrix on the basis of small angle neutron scattering as well as vibrational spectroscopy.[3−14] But one serious problem was encountered in the quantitative (or even qualitative) analysis of the aggregation state of D and H chains. For example, the blend between deuterated high-density polyethylene (DHDPE) and hydrogenated high-density PE (HDPE) was melted and cooled slowly to an ambient temperature. These two species or D and H chains were found to show phase segregation phenomenon; the D (or H) chains gather together in the H (or D) matrix.[5] This means that the evaluation of a radius of gyration of an individual chain is impossible. As will be described in the next paragraph, the almost perfect cocrystallization of the H and D chains in the crystal lattice was attained for the blend of DHDPE and LLDPE with about 17 ethyl branches/1000 carbon atoms, where LLDPE is a linear low-density PE of hydrogenous species.[13−19]

Polyethylene shows the splitting of infrared (and Raman) bands: for example, a pair of bands at 720 and 730 cm^{-1}, which is caused by an intermolecular correlation of vibrational modes between the neighboring zigzag chains included in the orthorhombic unit cell.[3,4,6,7,14] The band splitting width is dependent on the strength of vibrational coupling between the adjacent chains.[3,4] When the H chain stems are introduced to the unit cell of D chain stems, as illustrated in Figure 1, the vibrational coupling between the H chain stems is reduced since the CH_2 and CD_2 groups vibrate at appreciably different frequencies. As a result the band profile changes between doublet and singlet depending on the blend content. This is observed quite clearly for the mixture of *n*-$C_{36}H_{74}$ and *n*-$C_{36}D_{74}$,[6,7] indicating a random distribution of H and D stems in the crystal or the perfect cocrystallization phenomenon. The similar cocrystallization phenomenon is observed for the above-mentioned blend of DHDPE and LLDPE with a moderate degree of branching. The cocrystallization phenomenon can be observed also in the

* Corresponding author.
[†] Department of Future Industry-oriented Basic Science and Materials, Toyota Technological Institute.
[‡] Petrochemicals Research Laboratory, Sumitomo Chemical Co. Ltd.

10.1021/ma801824u CCC: $40.75
Published on Web 11/18/2008

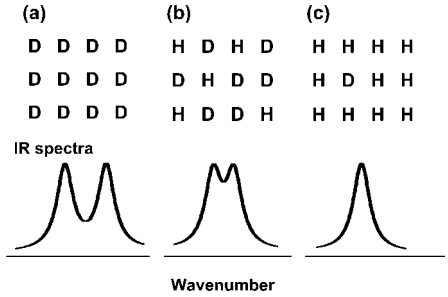

Figure 1. Schematic illustration of the aggregation state of hydrogenated (H) and deuterated (D) chain stems in the crystallite and the corresponding infrared spectral profiles of the D (or H) species.

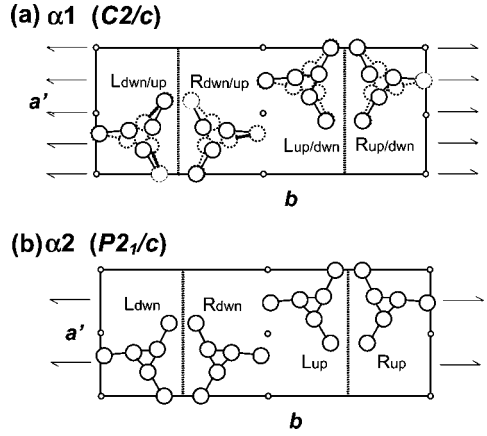

Figure 2. Crystal structure of iPP: (a) α1 form with statistically random packing of upward and downward chains (space group *C2/c*) and (b) α2 form with regular chain packing structure (space group $P2_1/c$).

systematic shift of the DSC peak corresponding to the melting (and crystallization) point of the crystals consisting of both the D and H chain stems. The systematic change in cocrystallization behavior indicates the random distribution of the chain stems, leading us to such a concept that the chain fold reentry must occur "randomly" for the melt-crystallized PE sample.[20] In this way the utilization of D/H blend samples is very useful for the investigation of the spatial distribution of the chain stems in the crystal lattice and the structural evolution process during the crystallization phenomenon.

In the present study, we choose isotactic polypropylene (iPP) as another target because of its importance in both scientific and industrial points of view. iPP has been widely used as a typical polymer for the studies of the crystallization from the melt,[21−33] shear-induced crystallization,[34−38] etc. because of its simple chemical structure and the polymer having helical chain conformation in the crystal lattice.[39] iPP crystallizes in four different crystalline modifications of monoclinic (α1, α2), trigonal (β), orthorhombic (γ) and hexagonal (smectic) systems.[40] Among them the disordered α1 form is generally obtained by slow cooling from the melt as shown in Figure 2 a. The α1 form exhibits the crystal structure of space group *C2/c* or *Cc*, in which the (3/1) helical chains with $(TG)_3$ conformation are packed upward and downward randomly at 50% probability, where T and G are *trans* and *gauch*e bonds, respectively.[39−42] When the α1 sample is annealed at higher temperature, it transforms to the α2 form with the structure shown in Figure 2 b, where the (3/1) helices are packed regularly upward and downward with the space group $P2_1/c$.[41,42] The γ form is obtained relatively easily for the iPP sample polymerized with the Ziegler−Natta catalyst under high pressure,[43,44] for the low-molecular weight compounds at atmospheric pressure[45,46]and for the ethylene-polypropylene copolymers.[47,48] The γ form can be also obtained from the iPP samples which are polymerized with metallocene catalyst system and contain the *regio* and *stereo* defects.[49,50]

Table 1. Characterization of iPP Samples

sample	M_w	M_w/M_n
hydrogenated iPP	160K	3.0
deuterated iPP	200K	2.5

As for the aggregation state of iPP chains in the α1 and α2 crystal lattices, we have still many unsolved problems. For example, if we trace a loop of a single chain in the crystallite, we have several possible routes: one chain is folded back to the adjacent point (adjacent reentry) or it returns into random position (random reentry). For clarifying this chain folding mode of iPP, the utilization of blend samples between H and D chains should be able to be helpful as likely the case of polyethylene mentioned above. In the case of iPP, the small-angle neutron scattering (SANS) data were reported for an H/D blend sample with 5 mol % D content, from which the random reentry model was proposed by Ballard et al.[51−53] Unfortunately, however, they did not show a clear experimental evidence to support the cocrystallization phenomenon between the H and D species of iPP, but they interpreted the SANS data by *assuming* a homogeneous distribution of D chain species in the H chain matrix. We need to establish the cocrystallization between the H and D species of iPP in more direct manner on the basis of other methodologies to clarify the concept of random distribution of the D and H chain stems in the crystal lattice. For this purpose we utilize the thermal and vibrational spectroscopic methods as described in the present paper. These two methods have been proved to be quite useful for the discussion of cocrystallization phenomenon as seen in the case of polyethylene.[8,9,13−20] We report here the DSC and infrared spectral data measured for a series of H/D blends samples with various H/D contents to show definitely the cocrystallization phenomenon. To the best of our knowledge, no report has been made at all about this theme of cocrystallization phenomenon in the iPP blends between H and D species on the basis of thermal and vibrational spectroscopic data. The SANS experiment reported that the D and H blends of it-PP cocrystallize for the sample with small portion of D species in the H matrix. We investigate the DSC and vibrational spectra for the samples with a wide range of H/D content to confirm the cocrystallization phenomenon for any blend samples of H and D iPP species. The clarification of the spatial distribution of the D and H chain stems should allow us to speculate about the chain folding mode in the crystalline lamellae. This type of discussion was mainly made by focusing polyethylene as one of the most typical polymers.[1] As pointed out by the late Dr. Keller,[1] however, we cannot generalize the results obtained for polyethylene only. We need to investigate the details of the aggregation state of iPP chains enough sufficiently. The present paper is to challenge this apparently outdated but even now important and unsolved problem from the new point of view.

Experimental Section

Samples. The samples used are listed in Table 1. The pure deuterated (D) and hydrogenated (H) isotactic polypropylene samples were obtained by polymerization of deuterated propene and hydrogenous propene, respectively, with a metallocene catalyst system. The molecular weights of the polymers were determined by high temperature gel permeation chromatography with *o*-dichlorobenzene as an eluent.

The blend samples of the H and D species of 0:100, 5:95, 25:75, 50:50, 75:25, 95:5 and 100:0 molar ratios were prepared by dissolving in boiling *p*-xylene at a concentration of 2 wt % under nitrogen atmosphere followed by precipitating into methanol at room temperature by vigorous stirring. The precipitated samples

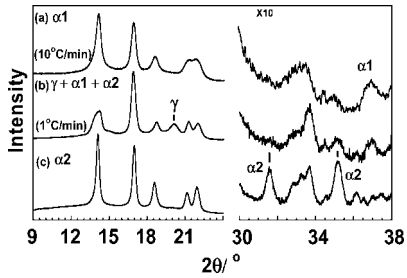

Figure 3. Wide angle X-ray diffraction profiles taken for different kinds of iPP samples: (a) sample prepared by cooling from the melt to room temperature at 10 °C/min (α1 form), (b) sample prepared by cooling from the melt to room temperature at 1 °C/min (mixture of α1, α2 and γ forms) and (c) the α2 sample prepared by annealing the α1 form at 154 °C for 4h.

were dried in a vacuum oven at 100 °C and cooled slowly to the room temperature. The physically mixed sample of D and H species was prepared by mixing the powder samples of these two species as homogeneously as possible by hand.

Thin films of the blend and pristine samples were prepared by slow cooling the melt under compression. The unoriented α1 samples were prepared by slow cooling from the melt at ca. 10 °C/min. The unoriented α1 sample was annealed at 154 °C for 4 h and quenched to ambient temperature to obtain highly-ordered α2 sample. The oriented films were prepared as follows: the unoriented (α1) films were cut into rectangular shape and were stretched about five times the original length at 100 °C. All these samples were annealed in silicone oil bath at 154 °C for 4 h and used for the measurements of polarized infrared spectra after rinsing with petroleum ether. In the present paper the blend sample with a certain H/D ratio is named H**; for example, H75 is the blend of 75 mol % H species and 25 mol % of D species. The identification of the α1 and α2 forms was made by measuring the X-ray diffraction patterns.

Measurements. The DSC thermograms were measured in the heating and cooling processes using a differential scanning calorimeter TA DSC Q1000 under nitrogen gas atmosphere. The polarized infrared spectra were measured using a Varian FTS 7000 FT-IR spectrometer with a wire grid polarizer at room temperature and 77 K using an Oxford cryostat of ZnSe windows with liquid N_2 as coolant. The resolution power was 0.5 cm^{-1}. The wide angle X-ray diffraction (WAXD) was measured for identifying the crystalline forms of the prepared samples, where diffractions profiles were collected in a reflection mode using a Rigaku/TTR III X-ray diffractometer with Cu−Kα line as an incident X-ray beam. The fiber diagrams of the oriented samples were obtained by using an R-AXIS VII (Rigaku, Japan) with an imaging plate (IP) as a detector. The 2-dimensional small angle X-ray scattering (SAXS) measurements were made by using a NANO-Viewer (Rigaku, Japan) with an imaging plate as a detector where the graphite-monochromated Cu−Kα line was used as an incident X-ray beam.

Results and Discussion

The samples used here were synthesized by using the metallocene catalyst system. There is a possibility such that these iPP samples can easily form the α1 form, α2 form or the mixture of α1, α2 and γ forms depending on the crystallization conditions. The WAXD patterns were measured to identify the crystal forms of the samples. The typical WAXD profiles measured for the α1, α2 and the mixture of γ, α1 and α2 forms of H50 samples are shown in Figure 3. By comparing the X-ray peaks, the γ, α1 and α2 crystal forms were characterized reasonably.[40,54−56] Figure 3 a is the X-ray profile obtained for the α1 form which was crystallized from the melt at the cooling rate of 10 °C/min to room temperature. By annealing the α1 sample at 154 °C (below the melting point) for 4 h and quenched to an ambient temperature, the sharp peaks at $2\theta = 32^o$, 35^o etc. are detected to confirm the highly-ordered α2 crystal modification. The sample cooled at 1 °C/min from the melt is the mixture of the γ ($2\theta = 20^o$), α1 and α2 forms as seen in Figure 3 b. We checked the crystal forms for all the iPP blend samples with H content of 0 to 100 %.

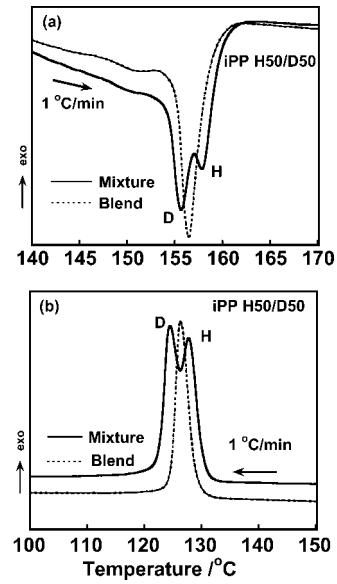

Figure 4. Comparison in the DSC thermogram between the blend of D/H 50 mol % ratio and the 50/50 physical mixture of the H and D species of iPP: (a) heating and (b) cooling processes.

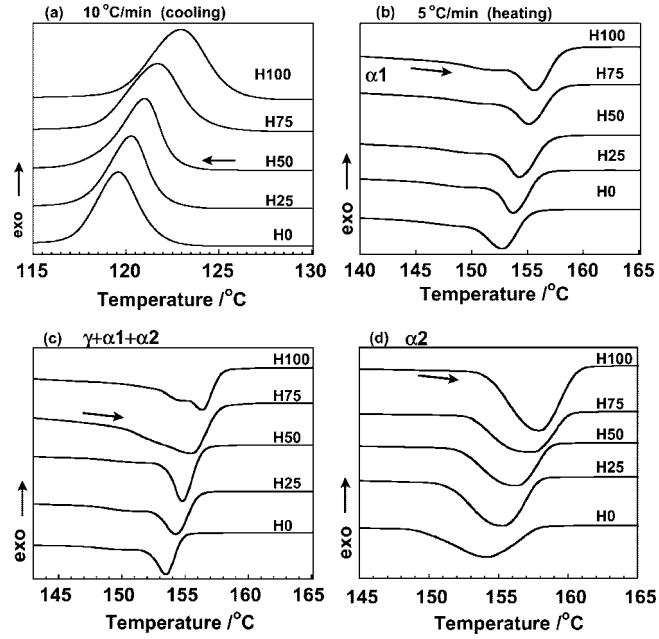

Figure 5. DSC thermograms of a series of iPP blend samples with various D/H contents. (a) Cooling processes from the melt at 10 °C/min, (b) the heating process starting from the α1 form (5 °C/min), (c) the heating process starting from the mixture of the α1, α2 and γ forms, and (d) the heating process starting from the α2 sample.

Thermal Analysis. In order to investigate the cocrystallization behavior of the iPP blends between the H and D species, we measured the DSC thermograms in the heating and cooling processes. Figure 4 a shows the DSC thermograms measured for the blend sample H50 and the corresponding mixture of pure H and D samples at 50/50 (H/D) ratio. A single melting peak is observed for H50 blend sample at a temperature between those of the original pure H and D samples. In the case of physical mixture of the H and D species the two melting points were

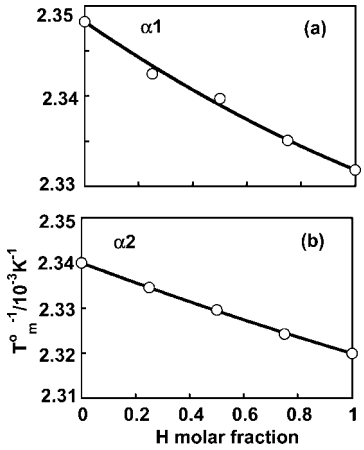

Figure 6. H content dependence of the melting point measured for a series of iPP blend samples: (a) α1 sample and (b) α2 sample. Open circle: the observed data and the solid line: the calculated result by eq 5 given in the text.

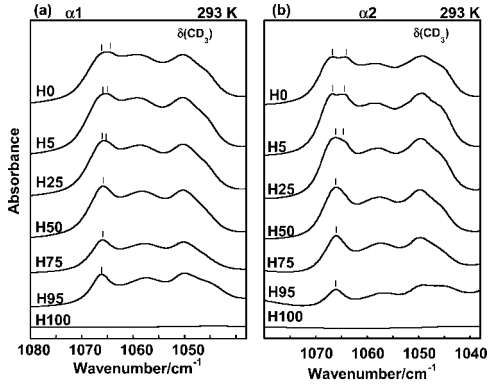

Figure 7. Infrared spectra in the CD_3 bending region at room temperature (293 K) measured for a series of unoriented iPP blend samples: (a) α1 and (b) α2 forms.

observed, corresponding to the melting peaks of the H and D species respectively. The similar observation was made also for the cooling process as shown in Figure 4 (b).

The DSC thermograms measured in the heating process for a series of blends are shown in Figure 5. Figure 5 a shows the exothermic peak measured for a series of H/D blend samples in the crystallization process from the melt. In this case the α1 form was obtained as identified by the WAXD measurements. The crystallization temperature is found to shift continuously toward higher temperature side with an increase of the H content during the α1 formation. As seen in Figure 5 b−d and Figure 6, for all the samples of α1 (Figure 5 b), α2 (Figure 5 d) and mixture of γ, α1 and α2 forms (Figure 5 c), the melting endothermic peak shift continuously toward higher temperature side with increasing the H content. Since the DSC thermograms of the mixtures of α1, α2, and γ forms are complicated, we will focus our discussion onto the α1 and α2 forms.

The continuous shift of melting temperature as a function of H/D ratio can be interpreted as follows.[20] If we assume a random distribution of H and D chains in the molten state of a blend, then the melting enthalpy ΔH and melting entropy ΔS may be expressed approximately by the following equations. Since the probabilities finding the H−H, D−D and H−D pairs in the blend are expressed by X^2, $(1\text{-}X)^2$ and $2X(1\text{-}X)$, respectively, where X is the molar ratio of the H species, then we have

$$\Delta H = X^2\Delta H_{hh} + (1-X)^2\Delta H_{dd} + 2X(1-X)\Delta H_{hd} \quad (1)$$

$$\Delta S = X^2\Delta S_{hh} + (1-X)^2\Delta S_{dd} + 2X(1-X)\Delta S_{hd} \quad (2)$$

where ΔH_{hh}, ΔH_{dd}, and ΔH_{hd} are the enthalpy changes related to the systems constructed by the H−H, D−D, and H−D pairs, respectively. At the melting point T_m, ΔH, and ΔS are related by the equation $\Delta H - T_m\Delta S = 0$.

Therefore

$$T_m = \frac{X^2\Delta H_{hh} + (1-X)^2\Delta H_{dd} + 2X(1-X)\Delta H_{hd}}{X^2\Delta H_{hh}/T^0_{mhh} + (1-X)^2\Delta H_{dd}T^0_{mdd} + 2X(1-X)\Delta S_{hd}} \quad (3)$$

where we utilized the relation of $\Delta H_{hh} = T^0_{mhh}\Delta S_{hh}$, and so on. Since the experimentally-observed melting enthalpy ΔH^{obs} is almost the same for all the samples within the experimental error, it might be reasonable to assume that $\Delta H_{hh} = \Delta H_{dd} = \Delta H_{hd}$. Then, from eq 3, we have

$$T^{obs}_m = \frac{1}{X^2/T^{obs}_m + (1-X)^2/T^{obs}_m + 2X(1-X)/T^0_{mhd}} \quad (4)$$

Substituting the observed data

$$1/T^{obs}_m = X^2/T^{obs}_m(H) + (1-X)^2/T^{obs}_m(D) + 2X(1-X)/T^0_{mhd} \quad (5)$$

Using eq 5, the experimental values of T^{obs}_m are fitted by choosing a parameter T^0_{mhd} as shown in Figure 6, where $T^0_{mhd} = 427.7$ K. Judging from the continuous shift in the melting peak as well as the crystallization point, it may be said clearly that almost the perfect cocrystallization occurs between the H and D species of iPP.

Infrared Spectra. *(1) Unoriented Samples.* To confirm the H/D cocrystallization phenomenon as revealed by the DSC data, we measured the infrared spectra for a series of the blend samples with the α1 and α2 crystalline forms. Figure 7 shows the infrared spectra measured at room temperature. The $\delta(CD_3)$ band or CD_3 bending mode observed in the 1080−1035 cm^{-1} region has been found to show the splitting for the pure D sample (H0), which is considered due to the correlation splitting in the crystal lattice, as will be discussed in a later section. The band splitting becomes clearer for the α2 sample than that of the α1 sample, reflecting the difference in the packing disorder in the latter case. It should be emphasized here that the band splitting width found for both the α1 and α2 samples becomes narrower with the decrease in D content and almost a singlet for the case of H95 sample. As seen in Figure 8, the $\delta(CD_3)$ mode at 1066 cm^{-1} shows clearer splitting at 77 K compared with the room temperature spectra in both the α1 and α2 samples. This band splitting at 77 K changed also continuously to the singlet for the H95 sample. Such a larger splitting width at low temperature may come from the cease of CD_3 rotational motions at low temperature, making the anisotropic intermolecular interactions more remarkable.[57−60] (It should be noticed here that the comparison in infrared spectral profile between the blend samples and the physically-mixed samples is useful for clarifying the change in splitting width observed for the blend samples. For example, we compare the spectra measured for the mixture of H0 and H100 α2 sample with the molar ratio 25/75 as shown in Figure 8, indicating a clear difference in the spectral profile between the blend and the mixture.)

The band splitting phenomenon may be interpretated reasonably by investigating the correlation table (Table 2).[58] An isolated chain of iPP takes the perfect 3/1 helical symmetry (C_3^s) and the corresponding factor group is isomorphous to the point group C_3. The normal modes are classified into two kinds of symmetry species A and E. The molecular chains packed in the crystal lattice do not possess any symmetry element except an identity element. The factor group of a chain in the crystal lattice is isomorphous to C_1 point group. Therefore the degeneracy of the E mode is eliminated and the corresponding E band splits into two (site group splitting). The vibrational modes of these chains of lower-symmetry are correlated each other by the symmetry operations requested by the space group $P2_1/c$-C_{2h}.

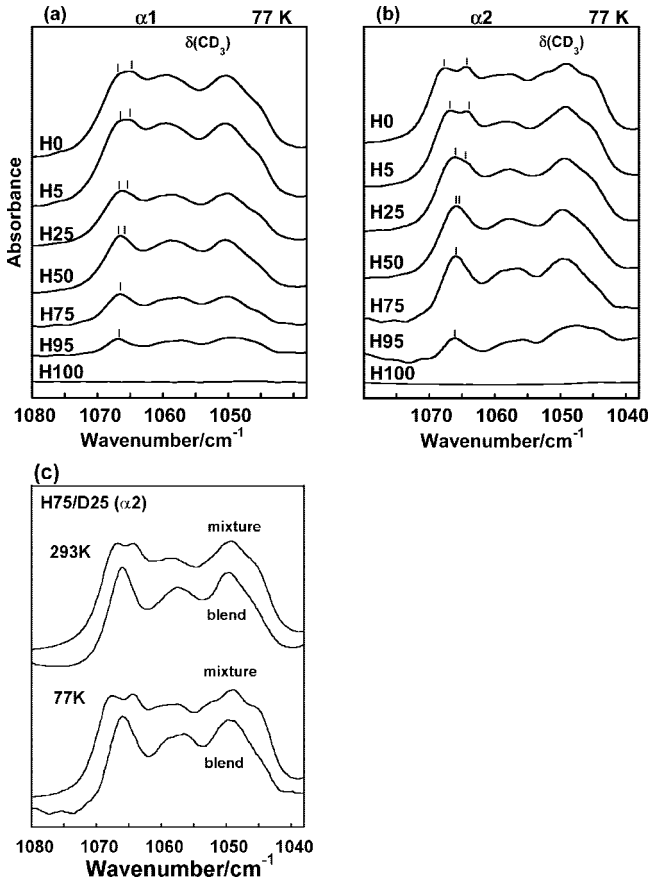

Figure 8. Infrared spectra in the CD_3 bending region at 77 K measured for a series of unoriented iPP blend samples: (a) α1 and (b) α2 forms. For comparison the infrared spectra measured for the blend and the physically-mixed samples of H75/D25 species (α2) are shown in part c to make the difference in infrared spectral profile between these two types of samples clearer.

Table 2. Correlation Table for iPP α2 Crystal

Molecular group symmetry (C_3)	Site group symmetry (C_1)	Space group symmetry (C_{2h})
A (//)	A	A_g (Raman)
		B_g (Raman)
E (⊥)		A_u (IR, ⊥)
		B_u (IR, //)

Since four chains are included in the unit cell, a molecular vibration may be classified to the four symmetry species (A_g, B_g, A_u, and B_u). The first two species are Raman active and the last two species are infrared active. That is, the vibrational modes are observed as a splitted pair of bands in both the infrared and Raman spectra. As said above, the originally-degenerated E mode is splitted into two bands due to the site group symmetry splitting, and each band is furthermore splitted into two by the symmetry correlation in the crystal lattice. Tashiro et al. performed the normal modes calculation for the α crystal form of iPP H species.[58] The calculated vibrational bands show the splitting of 0−7 cm^{-1} due to the site group splitting and 0−2 cm^{-1} due to the correlation splitting. The correlation splitting

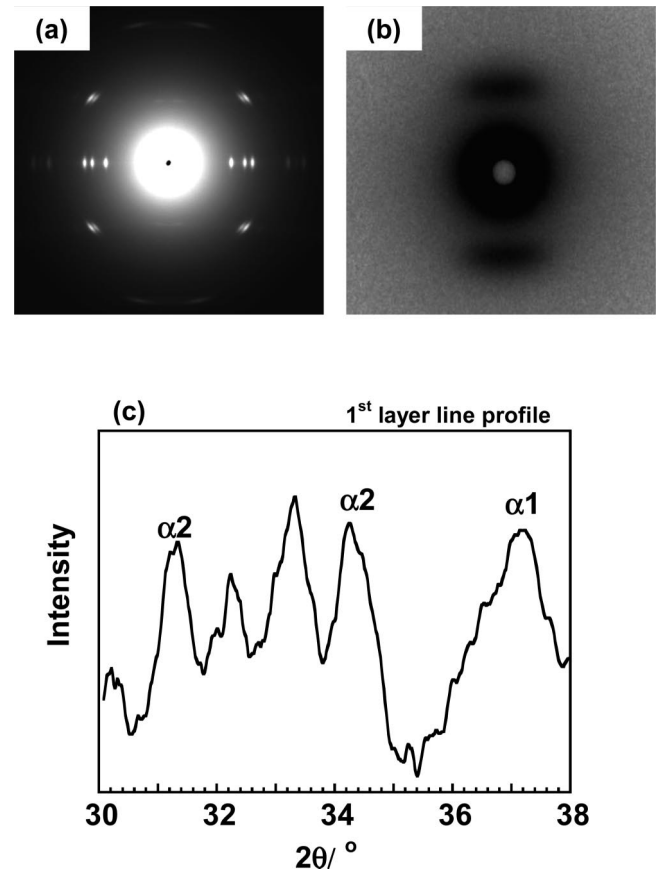

Figure 9. (a) 2D WAXD pattern of the oriented H50 sample measured at room temperature. (b) SAXS pattern of H50 oriented sample and (c) the first layer line profile to show the mixture of the α1 and α2 forms.

was not detected for the pure H sample even at 77 K because of too small splitting width. The correlation splitting was detected clearly and for the first time for the D species as seen in Figure 8. Such correlation splitting width is reduced by diluting the D chains with the H chains or due to the vibrational decoupling between the neighboring D chains, resulting in the singlet band observed for the H95 sample.

The vibrational modes of the α1 crystal modification are similar to those of the α2 form sample. In the case of α1 crystal form, however, the packing disorder of the upward and downward chains at the same lattice site may break such a vibrational correlation and the bands are predicted to split in a more complicated manner. Apparently broad band profile observed for the α1 form of the pure D sample may reflect such a situation (Figures 7 and 8).

(2) DSC and Infrared Data of Oriented Samples. Utilization of the polarized infrared spectra is useful for the interpretation of the complicated spectral profile. We prepared the oriented samples for a series of iPP D/H blends to confirm the band splitting due to the vibrational correlation between the neighboring chains in the crystal lattice. In order to do so, of course, we need to check the crystalline form of the oriented samples. As reproduced in Figure 9, the samples are found to be the mixtures of α1 and α2 forms. Figure 10 shows the polarized infrared spectra measured at 77 K for a series of the blend samples. The parallel polarized infrared band at 1066 cm^{-1} is splitted into two for the H0−H25 samples and it appears to be singlet for H50−H95 samples. The splitting width decreased continuously by decreasing the D chain concentration. As shown in Figure 11, the DSC thermograms were also measured for these oriented samples. The melting peak shifted continuously toward higher temperature side with increasing the H content. In this

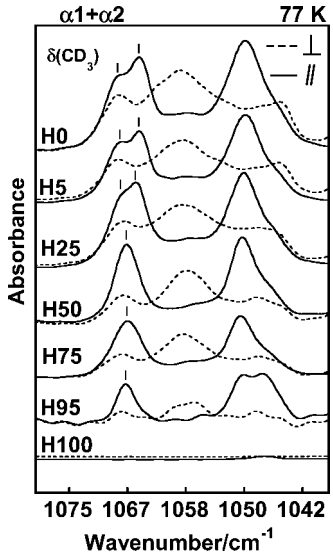

Figure 10. Polarized infrared spectra in the CD_3 bending region measured at 77 K for a series of uniaxially-oriented iPP blend samples with the various H contents. Solid line: the electric vector of an incident infrared beam parallel to the chain axis. Broken line: the electric vector of an incident infrared beam perpendicular to the chain axis.

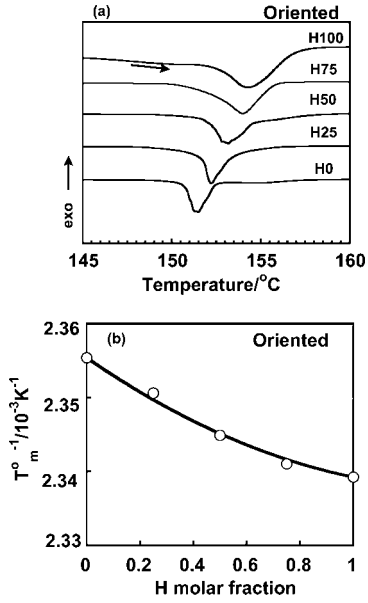

Figure 11. (a) DSC thermograms taken for a series of oriented iPP blend samples with various D/H contents measured in the heating process (5 °C/min). (b) The H content dependence of the melting point measured for the oriented iPP blend samples. Open circle: the observed data and solid line: the calculated result by eq 5 given in the text.

case also the melting points were reproduced reasonably using eq 5 under the assumption of random distribution of the H and D species in the crystal lattice ($T^0_{mhd} = 427.2$ K).

In this way, both the infrared spectra and DSC thermograms of the oriented samples with different H/D contents exhibit essentially the same phenomena as those observed for the unoriented samples. The oriented samples are the mixtures of the α1 and α2 forms, and the infrared band splitting and the DSC curves might be the averages of the α1 and α2 contributions. We may conclude reasonably that the H and D chain stems of iPP can cocrystallize almost perfectly when the samples are cooled from the molten state irrespective of the unoriented and oriented sample species. This can be said for both of the α1 and α2 crystals. The continuous shift in the melting point and the continuous decrease in the infrared band splitting width by

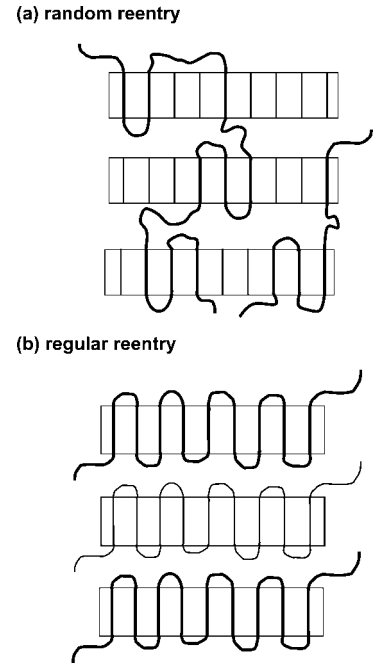

Figure 12. Schematic illustrations of (a) random reentry chain folding mode and (b) regular reentry mode.

dilution of D species with the H species confirm the concept of random distribution of the D and H chain stems in the crystal lattice as illustrated in Figure 1. This aggregation structure of the D and H chains can be kept even after the sample is deformed to the oriented sample.

It is possible in principle to estimate the spatial distribution of D and H stems in the crystallite from the quantitative data analysis of infrared band profile as reported by Krimm et al.[6,7] and Tashiro et al.[17,18] for the H/D blend samples of polyethylene. However, the spectral profile is more complicated for the case of it-PP blend samples since the correlation splitting and the site-group splitting contribute to the profile, and the packing disorder may also give additional splitting due to the symmetry lowering. Therefore it might be difficult to deduce a concrete image of spatial distribution of D and H stems of it-PP chains.

When we consider such an infrared band profile in more accurate manner, we may need to include the kinetic effect in the crystallization process from the melt. For the sample of higher H content, a fraction of crystallites with a higher concentration of H stems might be formed. As the crystallization proceeds furthermore the D and H chain stems are gathered together to be distributed randomly to form the major part of crystallites. The similar consideration was already made for the case of D/H blends of polyethylene in our previously published paper (refs 17 and 18): in the early stage of crystallization the H segments crystallize with the small portion of D species included and then the D and H stems are gathered together to form the whole crystallites. As a result the infrared band profile (and the DSC peak) become more or less complicated than those predicted for the perfectly statistically random distribution. Therefore, it is better to say at the present stage that the DSC and infrared spectra measured for a series of D/H blend samples allow us to have an image of statistically random spatial distribution of the H and D chain stems in a crystallite in a good and reasonable approximation.

The concept of random distribution of the D and H chain stems in the crystal lattice allows us to imagine that the chain folding should occur in a random reentry mode as illustrated in Figure 12 as long as the melt cooled samples are concerned with. This idea can be applied also to the oriented lamellar

structure. As seen in Figure 9 b, a meridional scattering is detected in the SAXS pattern of the oriented sample, indicating the repetition of crystalline and amorphous regions along the draw direction. The random distribution of the D and H chain stems is speculated to be kept even after stretching the unoriented H/D blend samples of the random chain folding structure. The morphology change of the stacked lamellae after necking is said to occur through the melt-recrystallization under the tensile force.[61] If it is true, we may say that the random H/D chain distribution is reserved even after the remarkably large morphological change occurs by melt-recrystallization.

Conclusions

In this paper, the cocrystallization behavior has been established successfully and for the first time for a series of blends between H and D species of isotactic polypropylene based on the analysis of DSC and infrared data. The continuous change in the melting and crystallization points and the infrared spectral profiles in $\delta(CD_3)$ region indicates a random distribution of the H and D chain stems in the crystalline lamella. This statistically random distribution of H and D chains naturally leads us to the building-up of the concept of a random reentry chain folding mode.

The results clarified in the present paper are considered to be important for the study of the crystallization behavior of iPP. As will be reported in a separate paper the crystallization rate of the H species is much slower than that of the D species during the isothermal crystallization when compared for the same degree of supercooling. In spite of this difference in the crystallization behavior, the cocrystallization can occur between the D and H species, probably as a result of sensitive balance between the kinetic and thermodynamic factors as already discussed for the case of isothermal crystallization of polyethylene D/H blend samples.[14−20]

Acknowledgment. This study was financially supported by a MEXT "Collaboration with Local Communities" project (2005−2009).

References and Notes

(1) A special issue on crystallization of polymers. , *Faraday Discuss. Chem. Soc.* **1979**, *68*000.
(2) *Proceedings of the NATO Advanced Research Workshops on Crystallization Process of Polymers*; Dasiere, M., Ed.; Series C; Kluwer Academic Publ.: Dordrecht, The Netherlands, 1993, *Vol. 405*.
(3) Tasumi, M.; Krimm, S. *J. Chem. Phys.* **1967**, *46*, 755.
(4) Tasumi, M.; Krimm, S. *J. Polym. Sci. Part A-2* **1968**, *6*, 995.
(5) Stehling, F. C.; Ergos, E.; Mandelkern, L. *Macromolecules* **1971**, *4*, 672.
(6) Krimm, S.; Ching, J. H. C. *Macromolecules* **1972**, *5*, 209.
(7) Bank, M. I.; Krimm, S. *J. Polym. Sci. Polym. Phys. Ed.* **1969**, *7*, 1785.
(8) Shelten, J.; Wignall, G. D.; Ballard, D. G. H. *Polymer* **1974**, *15*, 682.
(9) Shelten, J.; Ballard, D. G. H.; Wignall, G. D.; Longman, G. W.; Schmatz, W. *Polymer* **1974**, *15*, 682.
(10) Shelten, J.; Ballard, D. G. H.; Wignall, G. D.; Longman, G. W.; Schmatz, W. *Colloid Polym. Sci.* **1974**, *252*, 749.
(11) Shelten, J.; Ballard, D. G. H.; Wignall, G. D.; Longman, G.W.; Schmatz, W. *Polymer* **1976**, *17*, 751.
(12) Yoon, D. Y.; Flory, P. J. *Polymer* **1977**, *18*, 509.
(13) Macconnachie, A.; Richards, R.W. *Polymer* **1978**, *19*, 739.
(14) Tashiro, K.; Stein, R. S.; Hsu, S. L. *Macromolecules* **1992**, *25*, 1801.
(15) Tashiro, K.; Satkowski, M. M.; Stein, R. S.; Li, Y.; Chu, B.; Hsu, S. L. *Macromolecules* **1992**, *25*, 1809.
(16) Tashiro, K.; Izuchi, M.; Kobayashi, M.; Stein, R. S. *Macromolecules* **1994**, *27*, 1221.
(17) Tashiro, K.; Izuchi, M.; Kobayashi, M.; Stein, R. S. *Macromolecules* **1994**, *27*, 1228.
(18) Tashiro, K.; Izuchi, M.; Kobayashi, M.; Stein, R. S. *Macromolecules* **1994**, *27*, 1234.
(19) Tashiro, K.; Izuchi, M.; Kaneuchi, F.; Jin, C.; Kobayashi, M.; Stein, R. S. *Macromolecules* **1994**, *27*, 1240.
(20) Sasaki, S.; Tashiro, K.; Gose, N.; Imanishi, K.; Izuchi, M.; Kobayashi, M.; Imai, M.; Ohashi, M.; Yasuo, Y.; Ohayama, K. *Polym. J.* **1999**, *31*, 677.
(21) Padden, F. J.; Keith, H. D. *J. Appl. Phys.* **1959**, *30*, 1479.
(22) Keith, H. D.; Padden, F. J. *J. Appl. Phys.* **1964**, *35*, 1270–1286.
(23) Padden, F. J.; Keith, H. D. *J. Appl. Phys.* **1966**, *37*, 4013.
(24) Lovinger, A. J. *J. Polym. Sci., Polym. Phys. Ed.* **1983**, *21*, 97.
(25) Norton, D. R.; Kellar, A. *Polymer* **1985**, *26*, 704.
(26) Lotz, B.; Wittmann, J. C. *J. Polym., Polym. Phys. Ed.* **1986**, *24*, 1541.
(27) Olley, R. H.; Bassett, D. C. *Polymer* **1989**, *30*, 399.
(28) Okada, T.; Saito, H.; Inoue, T. *Macromolecules* **1992**, *25*, 1908.
(29) Ryan, A. J.; Terrill, N. J.; Fairclough, J. P. A. *ACS PMSE Prepr.* **1998**, *79*, 358.
(30) Terrill, N. J.; Fairclough, P. A.; Towns-Andrews, E.; Komanschek, B. U.; Young, R. J.; Ryan, A. J. *Polymer* **1998**, *39*, 2381.
(31) Iijima, M.; Strobl, G. *Macromolecules* **2000**, *33*, 5204.
(32) Heeley, E. L.; Maidens, A. V.; Olmsted, P. D.; Bras, W.; Dolbnya, I. P.; Fairclough, J. P. A.; Terrill, N. J.; Ryan, A. J. *Macromolecules* **2003**, *36*, 3656.
(33) De Rosa, C.; Auriemma, F.; Resconi, L. *Macromolecules* **2005**, *38*, 10080.
(34) Kumaraswamy, G.; Issaian, A. M.; Kornfield, J. A. *Macromolecules* **1999**, *32*, 7537.
(35) Somani, R. H.; Hsiao, B. S.; Nogales, A.; Srinivas, S.; Tsou, A. H.; Sics, I.; Balta-Calleja, F. J.; Ezquerra, T. A. *Macromolecules* **2000**, *33*, 9385.
(36) Kumaraswamy, G.; Kornfield, J. A.; Yeh, F.; Hsiao, B. *Macromolecules* **2002**, *35*, 1762.
(37) Somani, R. H.; Yang, L.; Hsiao, B. S.; Agarwal, P. K.; Fruitwala, H. A.; Tsou, A. H. *Macromolecules* **2002**, *35*, 9096.
(38) Li, L.; De Jeu, W. H. *Phys. Rev. Lett.* **2004**, *92*, 75506.
(39) Natta, G.; Corradini, P. *Nuovo Cimento Suppl.* **1960**, *15*, 40.
(40) Brückner, S.; Meille, S. V.; Petraccone, V.; Pirozzi, B. *Prog. Polym. Sci.* **1991**, *16*, 361.
(41) Mencik, Z. *J. Macromol. Sci., Phys* **1972**, *B6*, 101.
(42) Hikosaka, M.; Seto, T. *Polym. J.* **1973**, *5*, 111.
(43) Pae, K. D.; Sauer, J. A.; Morrow, D. R. *Nature* **1966**, *211*, 514.
(44) Mezgahni, K.; Philiphs, P. J. *Polymer* **1997**, *38*, 5725.
(45) Morrow, D. R.; Newman, B. A. *J.Appl. Phys.* **1968**, *39*, 4944.
(46) Lotz, B.; Graff, S.; Wittman, J. C. *J. Polym. Sci., Polym Phys. Ed.* **1986**, *24*, 2017.
(47) Turner-Jones, A. *Polymer* **1971**, *12*, 487.
(48) Mezgahni, K.; Philiphs, P. J. *Polymer* **1995**, *36*, 2407.
(49) Fischer, D.; Mulhaupt, R. *Macromol. Chem. Phys.* **1994**, *195*, 1433.
(50) Alamo, R. G.; Man-Ho, K.; Maria, J. G.; Jose, R. I.; Mandelkern, L. *Macromolecules* **1999**, *32*, 4050.
(51) Ballard, D. G. H.; Cheshire, P.; Longman, G. W.; Schelten, J. *Polymer* **1978**, *19*, 379.
(52) Ballard, D. G. H.; Longman, G. W.; Cowley, T. L.; Cunningham, A.; Schelten, J. *Polymer* **1979**, *20*, 399.
(53) Ballard, D. G. H.; Burgess, A. N.; Nevin, A.; Cheshire, P.; Longman, G. W.; Schelten, J. *Macromolecules* **1980**, *13*, 677.
(54) Auriemma, F.; De Ballesteros, O. R.; De Rosa, C.; Corradini, P. *Macromolecules* **2000**, *33*, 8764–8774.
(55) Radhakrishnan, J.; Ichikawa, K.; Yamada, K.; Toda, A.; Hikosaka, M. *Polymer* **1998**, *39*, 2995–2997.
(56) De Rosa, C.; Guerra, G.; Napolitano, R.; Pettraccone, V.; Pirozzi, B. *Eur. Polym. J.* **1984**, *20*, 937–941.
(57) Ishida, Y.; Yamafuji, K.; Koll, Z. Z. *Polymer* **1961**, *177*, 97.
(58) Tashiro, K.; Kobayashi, M.; Tadokoro, H. *Polym. J.* **1992**, *24*, 899.
(59) Beckett, D. R.; Chalmers, J. M.; Mackenzie, M. W.; Willis, H. A.; Edwards, H. G. M.; Lees, J. S.; Long, D. A. *Eur. Polym. J.* **1985**, *21*, 849–852.
(60) Fraser, G. V.; Hendra, P. J.; Watson, D. S.; Gall, M. J.; Willis, H. A.; Cudby, M. E. A. *Specrtrochim. Acta* **1978**, *29*, 1525–1533.
(61) Pope, D. P.; Keller, A. *J. Polym. Sci., Polym. Phys. Ed.* **1975**, *12*, 533.

MA801824U